*Manuscript
Click here to download Manuscript: ICSSP4-v2.doc Click here to view linked References

The Prediction of Tip Radius During Rapid Dendritic Growth Under Coupled Thermo-Solutal Control: What Value σ^*

A.M. Mullis[§], J. Rosam[§,‡] & P.K. Jimack[‡]*

Institute for Materials Research[§] and School of Computing[‡],
University of Leeds, Leeds LS2 9JT, UK.

* Corresponding Author: email: a.m.mullis@leeds.ac.uk;
fax : +44 113 343 2384
tel : +44 113 343 2568

Key Words: Rapid solidification, Phase-field modelling, Dendritic Growth

Abstract

A phase-field model for dendritic growth under coupled thermo-solutal control model is presented. Constructed in the quantitatively valid thin-interface limit the model uses advanced numerical techniques such as mesh adaptivity, multigrid and implicit time-stepping to solve the non-isothermal alloy solidification problem for materials parameters that are realistic for metals. Using this model we demonstrate that the dendrite radius selection parameter, σ^*, shows a complex dependence on a number of materials properties including undercooling, Lewis number, alloy concentration and partition coefficient, in addition to the known dependence on anisotropy strength. Consequently, we argue that as a predictive tool, at least for non-isothermal alloy solidification away from the limits of vanishing concentration and Peclet number, the concept of σ^* probably retains little intrinsic value.

Introduction

One of the most powerful techniques to emerge in recent years for modelling solidification microstructures is the phase-field method. By assuming the solid-liquid interface to be diffuse, a continuous (differentiable) order parameter, ϕ, may be defined which represents the phase of the material. The evolution of ϕ is governed by a free energy functional which can be solved using standard techniques for PDEs, avoiding the need to explicitly track the solid-liquid interface and thus allowing the simulation of arbitrarily complex morphologies. Consequently, most solidification structures, including dendrites[1], eutectics[2], peritectics[3] and monotectics[4] have been simulated via this method. The technique has been subjected to careful validation against experiment, specifically in relation to dendrite growth velocities and tip radii, with good agreement being shown between phase-field models and the most carefully conducted dendrite growth experiments undertaken as part of the US Isothermal Dendrite Growth Experiment II[5], performed in microgravity conditions.

As a result, phase-field modelling is now the technique of choice for simulating solidification microstructures, with numerous notable examples of its success. These include the inclusion of flow effects[6] and electric currents[7] in the solidifying melt, elucidating the mechanisms behind long-standing problems in solidification such as spontaneous grain refinement[8] and twinned dendritic growth[9] and predicting the effect of external oscillating fields on dendrites[10].

However, phase-field modelling presents significant computational challenges in that the resulting set of PDE's is highly non-linear and generally the width of the diffuse interface must be much narrower than the smallest physical feature to be simulated. This results in very large computational meshes. Consequently, most phase-field models employ a restrictive set of assumptions wherein, with only a very few exception, the models are constructed within the idealized limit that solidification is controlled by the diffusion of one species only, either heat or solute. While true for the thermally controlled solidification of pure elements, in alloy systems it requires one to assume that growth is so slow that the system remains everywhere isothermal, an assumption that is hard to justify during rapid solidification processing operations such as gas and centrifugal atomisation, melt spinning, planar flow casting, laser surface melting and many welding techniques.

To date, relatively few attempts have been made to use phase-field techniques to simulate coupled thermo-solutal solidification due to the severe multi-scale nature of the problem (typically Lewis number, $Le = \alpha/D$, is $10^3 - 10^4$, where α and D are the thermal and solutal diffusivities respectively). By extending the solutal model of Warren & Boettinger[11], Loginova *et al.*[12] have demonstrated such a model, although they were unable to eliminate the effects of the domain boundary on the thermal field. The methodology was subsequently extended by the introduction an adaptive finite volume solver[13], allowing realistic values of *Le* to be used without domain boundary effects being encountered. However, serious doubts have been raised regarding the quantitative validity of this model[14] as the numerical results appear to suggest excess solute trapping and have an unresolved interface width dependence. However, these problems may be overcome if the model is constructed within the thin interface limit, as first demonstrated by Karma[15]. Such a model of coupled thermo-solutal solidification has been formulated by Ramirez & Beckermann[14, 16] and subsequently

extended by ourselves[17, 18, 19] to include the application of advanced numerical techniques such as mesh adaptivity, implicit time discretisation and a multigrid solver which has permitted the model to be extended to Lewis numbers that are realistic for metallic melts[19]. As the thin interface model has been shown to be independent of the length scale chosen for the mesoscopic diffuse interface width, it is capable of giving quantitatively correct predictions for the velocity, V, and radius of curvature at the tip, ρ, during dendritic growth, permitting one of the longest standing problems in solidification theory to be tackled directly.

Analytical solutions[20] to the equations for dendritic growth predicted that it is the dimensionless Peclet number, $Pt = V\rho/2\alpha$, that is related to undercooling, ΔT, during growth, leading to a degeneracy in the product $V\rho$ not observed in nature. Various models based on the stability of the solidification front as it grows into its parent melt have been proposed[21, 22] to break this degeneracy (marginal stability), all of which contain a constant, σ^*, which arises from the stability analysis, and which may be equated with the group

$$\sigma^* = \frac{2\alpha d_o}{\rho^2 V}$$

where d_0 is the chemical capillary length. For a planar interface σ^* takes the value[21] $1/(4\pi^2) \approx 0.0253$, while similar values have been found for other shapes, including 2- and 3-D parabolic needles[23]. The apparent validity of these models was supported by the direct simultaneous measurement of V and ρ for succinonitrile[24] which yielded an experimental value for σ^* in this system of 0.0195, in close agreement with theory.

However, all such stability arguments were shown to be flawed by the application of boundary integral methods (microscopic solvability theory) which established that it is crystalline anisotropy[25] rather than stability *per se* that is responsible for breaking the degeneracy and therefore the apparent agreement between marginal stability theory and experiment is fortuitous. The full analysis reveals that in the limit of vanishing Peclet number an equation similar to the one arising from marginal stability is encountered but that σ^* is the anisotropy-dependant eigenvalue for the problem, which for small Peclet numbers is found to vary as $\sigma^*(\varepsilon) \propto \varepsilon^{7/4}$, where ε is a measure of the anisotropy strength.

As such there remains some validity in retaining the idea of σ^* as a stability 'constant', in that its value depends upon only one quantity, and moreover a quantity that generally appears nowhere else in the governing equations. However, both (numerical) solvability theory and phase field modelling of pure thermal growth have shown[26] that for finite Peclet number σ^* is a function of Pt, or equivalently, undercooling, with σ^* decreasing monotonically with increasing Pt. In this paper, focusing on phase-field models of coupled thermo-solutal solidification, we review the known dependencies of σ^* and present new data relating to the variation of σ^* with concentration. On the basis of the often very complex dependencies exhibited by σ^* we ask whether the idea of a stability parameter is worth retaining.

Description of the Model

The model adopted here is based upon that of [14] in which, following non-dimensionalization against characteristic length and time scales, W_0 and τ_0, the evolution of the phase-field, ϕ, and the dimensionless concentration and temperature fields U and θ are given by

$$A^2(\psi)\left[\frac{1}{Le}+Mc_\infty\left[1+(1-k_E)U\right]\right]\frac{\partial\varphi}{\partial t}=\nabla\cdot\left(A^2(\psi)\nabla\varphi\right)+\varphi(1-\varphi^2)$$
$$-\lambda(1-\varphi^2)^2(\theta+Mc_\infty U)-\frac{\partial}{\partial x}\left(A(\psi)A'(\psi)\frac{\partial\varphi}{\partial y}\right)+\frac{\partial}{\partial y}\left(A(\psi)A'(\psi)\frac{\partial\varphi}{\partial x}\right)$$

$$\left(\frac{1+k_E}{2}-\frac{1-k_E}{2}\varphi\right)\frac{\partial U}{\partial t}=\nabla\cdot\left(D\frac{1-\varphi}{2}\nabla U+\frac{1}{2\sqrt{2}}\left|1+(1-k_E)U\right|\frac{\partial\varphi}{\partial t}\frac{\nabla\varphi}{|\nabla\varphi|}\right)+\frac{1}{2}\left(\left|1+(1-k_E)U\right|\frac{\partial\varphi}{\partial t}\right)$$

$$\frac{\partial\theta}{\partial t}=\alpha\nabla^2\theta+\frac{1}{2}\frac{\partial\varphi}{\partial t}$$

where, for 4-fold growth, $A(\psi) = 1 + \varepsilon.\cos(4\psi)$, ψ is the angle between the principal growth direction and the local, outward pointing normal to the solid-liquid interface, k_E is the partition coefficient L and c_p are the latent and specific heats respectively and λ is a coupling parameter given by $\lambda = D/a_2 = a_1W_0/d_0$ with a_1 and a_2 taking the values $5\sqrt{2}/8$ and 0.6267 respectively [15] . U and θ are related to physical concentration, c, and temperature, T, via

$$U=\frac{1}{1-k_E}\left(\left(\frac{2c/c_\infty}{1+k_E-(1-k_E)\varphi}\right)-1\right)\quad\text{and}\quad\theta=\frac{\Delta T-mc_\infty}{L/c_p}\ ,$$

where m is the slope of the liquidus line, which has dimensionless form

$$M=\frac{|m|(1-k_E)}{L/c_p}\ .$$

The governing equations are descritized using a finite difference approximation based upon a quadrilateral, non-uniform, locally-refined mesh with equal grid spacing in both directions. This allows the application of standard second order central difference stencils for the calculation of first and second differentials, while a compact 9-point scheme has been used for Laplacian terms, in order to reduce the mesh induced[27] anisotropy. To ensure sufficient mesh resolution around the interface region and to handle the extreme multi-scale nature of the problem at high Lewis number local mesh refinement (coarsening) is employed when the weighted sum of the gradients of ϕ, U and θ exceeds (falls below) some predefined value.

It has been shown elsewhere that if explicit temporal descretization schemes are used for this problem the maximum stable time-step is given by $\Delta t \le Ch^2$, where $C = C(\lambda, Le, \Delta T)$, with C varying from ≈ 0.3 at $Le = 1$ to $C \le 0.001$ at $Le = 500$[17], leading to

unfeasibly small time-steps at high Lewis number. Consequently, an implicit temporal descretization is employed here based on the second order Backward Difference Formula with variable time-step.

When using implicit time discretisation methods it is necessary to solve a very large, but sparse, system of non-linear algebraic equations at each time-step. Multigrid methods are among the fastest available solvers for such systems and in this work we apply the non-linear generalization known as FAS (full approximation scheme [28]). The local adaptivity is accommodated via the multilevel algorithm originally proposed by Brandt[29]. The interpolation operator is bilinear while injection is used for the restriction operator. For smoothing the error we use a fully-coupled nonlinear weighted Gauss-Seidel iteration where the number of pre- and post-smoothing operations required for optimal convergence is determined empirically[17]. Full details of the numerical scheme are given in [17, 18, 30].

We obtain from the model the two key parameters characteristic of dendritic growth, namely the velocity and radius of the tip. The latter we obtain by fitting a parabolic profile to the $\phi = 0$ isoline using a 4th order interpolation scheme described in [17, 18], as this has generally been felt[14, 31] to be more directly comparable to analytical dendrite growth theories[22] , than the curvature directly from the derivatives of ϕ at the tip.

In order to compare our results with analytical theories of solidification it is also useful to be able to calculate the radius selection parameter, σ^*. In this respect we mean that we will use the values of V and ρ obtained directly from the phase-field model to calculate a value of σ^* such that, if one were to use a marginal stability model of dendritic growth with the given value of σ^*, the correct values of the velocity and radius would be recovered. The analysis is repeated separately at each undercooling for which the phase-field model is run as we do not assume that σ^* will necessarily remain constant. Specifically, the calculation of σ^* is such that V and ρ are recovered when the LKT[22] model of solidification with corrections for high undercoolings is used, wherein ρ is given by

$$\rho = \frac{d_0}{\sigma^* \left[\xi_{\mathrm{T}} Pt + 2\xi_c Pc \frac{|m| c_\infty}{L / c_p} \left(\frac{1-k_E}{1-(1-k_E)\Delta c} \right) \right]}$$

with

$$\xi_{\mathrm{T}} = 1 - \frac{1}{\sqrt{1 + \frac{1}{\sigma^* Pt^2}}} \quad ,$$

$$\xi_c = 1 + \frac{2k_E}{1 - 2k_E - \sqrt{1 + \frac{1}{\sigma^* Pc^2}}} \quad ,$$

where Pc is the solutal Peclet number (as distinct from the thermal Peclet number, Pt which has already been defined above) and Δc is the local concentration 'frozen in' at the interface (taken as $\phi = 0$) and which can be obtained directly from the phase-field simulation. This methodology was originally proposed by [14] and is explained in more detail in [18].

Results

The dependence of σ^* on undercooling[18] (at fixed concentration and Lewis number of $Mc_\infty = 0.05$ and $Le = 200$ respectively) and Lewis number[19] (at fixed undercooling and concentration of $\Delta = 0.15$ and $Mc_\infty = 0.05$ respectively) is summarised in Figures 1 & 2. In both cases significant variations in σ^* are observed, with this variation typically being around a factor of 2 with undercooling and a factor of 3 with Lewis number. Moreover, the variation is quite complex, particularly in the case of undercooling where σ^* displays both a local minimum and a local maximum.

Although this interpretation is somewhat speculative at the moment we note that the general form of the dependence of σ^* upon Δ observed in Figure 1, namely an initial decrease with increasing undercooling, giving way to a local minimum which is then followed by an increase, a local maximum and finally a further decrease, is actually very similar to the dependence predicted for ρ (upon Δ) by marginal stability models when σ^* is held constant. In this latter case the accepted interpretation is that we are seeing a transition in the mechanism controlling growth from solutal to thermal. Generally, for constant σ^*, ρ is predicted to decrease with increasing Peclet number. During coupled thermo-solutal growth the local minimum marks the onset of the transition from solutal growth at high solute Peclet number to thermal growth at low thermal Peclet number, while the maximum represent the transition to fully thermally controlled growth at moderate thermal Peclet number, wherein there is a decrease as the thermal Peclet number is increased further. However, as pointed out above, both (numerical) solvability theory and phase field modelling of pure melts have shown[26] σ^* decreasing monotonically with increasing Pt. Here we suggest that where there is more than one diffusing species (solute & heat) the competition between solutal and thermal growth mechanisms may manifest itself not necessarily in the radius, but in σ^*, giving rise to the complex behaviour observed.

In Figure 3 further investigation into the dependence of σ^* on concentration is presented at four different undercoolings between $\Delta = 0.4$ and $\Delta = 0.6875$. Again, significant variations in σ^* are observed which are quite complex in character. At the lowest undercooling displayed ($\Delta = 0.4$), and indeed for undercoolings below this level, a smooth decrease in σ^* is observed as the concentration is increased before a shallow local minimum is encountered around $Mc_\infty = 0.07$ (this feature not being present at lower undercoolings). With a small increase in the undercooling to $\Delta = 0.4625$ the curve retains largely the same form but there is now a distinct shoulder beginning to develop around $Mc_\infty = 0.03$, and with a further increase to $\Delta = 0.5875$ this becomes fully developed into a local maximum, while the local minimum observed around $Mc_\infty = 0.07$ at the two lower undercoolings is no longer evident. Finally, at the highest undercooling studied, $\Delta = 0.6875$, we observe a pronounced local maximum that is also shifted towards a higher concentration around $Mc_\infty = 0.05$. As in our previous investigations there is a variation in σ^* of around a factor of 3.

Moreover, for $\Delta = 0.4625$ a variation of this order is observed just with concentration (i.e. at fixed undercooling). Again, this variation would be consistent with a competition between solutal and thermally controlled growth mechanisms.

Although given the kind of complex quantitative model described here it is possible to calculate ρ (and indeed σ^*) directly, in many fields of solidification science a rather quick and crude estimate of characteristic dendrite length scales are required, and for this the approach often employed is to utilise an analytical approximation, such as the LKT[22] model, with some assumed constant value for σ^*, possibly one obtained from solvability theory in the low Peclet number limit for some assumed anisotropy. This theme is explored in Figure 4 where we plot the equivalent parabolic radius of curvature for our phase-field dendrites and in Figure 5 where we compare this with the corresponding radius estimated from LKT theory based on a σ^* which is constant with concentration. Here for each of the 4 undercoolings presented we have used the value of σ^* obtained from the phase-field model at $Mc_\infty = 0.02$ as the input value to the LKT model (and as a consequence the ratio between actual and LKT radius at $Mc_\infty = 0.02$ is by definition 1). However, this does give an inherent temperature variation to σ^* and were we to have used a value that was constant across all the simulations (i.e. constant with both concentration and undercooling) even larger variations would have been observed. Nonetheless, the ratio between actual (phase-field) and LKT radius of curvature is telling. At the lowest undercooling ($\Delta = 0.4$) the radius calculated assuming a constant σ^* shows a maximum difference of around 40% relative to that actually calculated from the phase-field model while at the highest undercooling ($\Delta = 0.6875$) this variation is almost a factor of 4. Indeed, at high undercooling the results here suggest one would actually introduce a smaller (although still substantial) error by assuming ρ to be constant, rather than σ^*.

Discussion

Given the results presented above and elsewhere by ourselves[17, 18, 19] and others[14, 16] it therefore becomes pertinent to ask what value there is retaining the notion of σ^* as a predictive tool, certainly for rapid solidification where the dendrite grows under coupled thermo-solutal control. To date it is already established that $\sigma^* = \sigma^*(\varepsilon, Le, \Delta, Mc_\infty)$ and although it is not a theme we have addressed in this paper one preliminary result suggests that k_E can also be added to the list of dependencies, with σ^* increasing by a factor of 1.6 (from 0.0200 to 0.0322) as k_E is increased from 0.15 to 0.30 (with $\Delta = 0.15$, $Mc_\infty = 0.05$, $\varepsilon = 0.02$). Moreover, in many cases it is a complex, non-monotonic variation that has been uncovered, and as the results presented here show, the interdependence between the variables is not easily separated, with increasing concentration giving possibly either a local minimum *or* a local maximum depending on undercooling. Under these circumstances we would therefore argue that as a predictive tool for rapid alloy solidification σ^* adds little. While it may retain a conceptual value at vanishing concentration and Peclet number, away from this limit σ^* has become a quantity we calculate once we know the dendrite tip radius rather than as means for calculating that radius.

References

[1] Mullis A M, *Phys. Rev. E* **68** (2003) 011602.

[2] Green J R, Mullis A M, and Jimack P K, *Metall. Mater. Trans. A* **38** (2007) 1426.

[3] Folch R, and Plapp M, *Phys. Rev. E* **72** (2005) 011602.
[4] Nestler B, Wheeler A A, Ratke L, and Stocker C, *Physica* **D 141** (2000) 133.
[5] Tennerhouse L A, Koss M B, LaCombe J C, and Glicksman M E, *J. Cryst. Growth* **174** (1997) 82.
[6] Lu Y, Beckermann C, and Ramirez J C, *J. Cryst Growth* **280** (2005) 320.
[7] Brush L N, *J. Cryst. Growth* **247** (2003) 587.
[8] Mullis A M, and Cochrane R F, *Acta Mater.* **49** (2001) 2205.
[9] Mullis A M, *Proc. 5th Decennial Conf. on Solidification Processing (SP2007)*, 23-25 July 2007, University of Sheffield, pp. 126-129. ISBN 095225074-8.
[10] Borzsonyi T, Toth-Katona T, Buka A and Granasy L, *Phys. Rev. Lett.* **83** (1999) 2853.
[11] Warren J A and Boettinger W J, *Acta metall. mater.* **43** (1995) 689.
[12] Loginova I, Amberg G, and Aagren J, *Acta mater.* **49** (2001) 573.
[13] Lan C W, Chang Y C, and Shih C J, *Acta mater.* **51** (2003) 1857.
[14] Ramirez J C and Beckermann C, *Acta mater.* **53** (2005) 1721.
[15] Karma A, *Phys. Rev. Lett.* **87** (2001) 115701.
[16] Ramirez J C and Beckermann C, *Phys. Rev. E* **69** (2004) 051607.
[17] Rosam J, PhD Thesis, University of Leeds, 2007.
[18] Rosam J, Jimack P K and Mullis A M, *Acta Mater.* **56** (2008) 4559.
[19] Rosam J, Mullis A M and Jimack P K, *Phys. Rev. E* **79** (2009) 030601.
[20] Ivantsov G P, *Doklady Akademii Nauk SSSR* **58** (1947) 567.
[21] Mullins W W and Sekerka R F, *J. Appl. Phys.* **33** (1964) 444.
[22] Lipton J, Kurz W and Trivedi R, *Acta Metall.* **35** (1987) 957.
[23] Langer J S and Muller-Krumbhaar H, *Acta. Metall.* **26** (1978) 1681.
[24] Huang S C and Glicksman M E, *Acta Metall.* **29** (1981) 701.
[25] Kessler D A, Koplik J and Levine H, *Adv. Phys.* **37** (1988) 255.
[26] Karma A and Rappel W-J, *Phys. Rev. E* **57** (1998) 4323.
[27] Mullis A M, *Comp. Mater. Sci.* **36** (2006) 345.
[28] Trottenberg U, Oosterlee C and Schuller A, *Multigrid*, Academic Press (2001).
[29] Brandt A, *Math. Comp.* **31** (1977) 333.
[30] Rosam J, Jimack P K and Mullis A M, *J. Comp. Phys.* **225** (2007) 1271.
[31] X. Tong, C. Beckermann, A. Karma, & Q. Li, Phys. Rev. E **63**, R49 (2001).

Figure Captions

Fig. 1. Radius selection parameter, σ^*, as a function of undercooling, Δ, for a non-isothermal alloy solidification model with $Mc_\infty = 0.05$, $Le = 200$, $k_E = 0.3$ and $\varepsilon = 0.02$.

Fig. 2. Radius selection parameter, σ^*, as a function of Lewis number, Le, for a non-isothermal alloy solidification model with $Mc_\infty = 0.05$, $\Delta = 0.15$, $k_E = 0.3$ and $\varepsilon = 0.02$.

Fig. 3. Radius selection parameter, σ^*, as a function of Mc_∞ for a non-isothermal alloy solidification model with $k_E = 0.3$ and $\varepsilon = 0.02$.

Fig. 4. Dendrite tip radius (parabolic), ρ_{para}, as a function of Mc_∞ for a non-isothermal alloy solidification model with $k_E = 0.3$ and $\varepsilon = 0.02$.

Fig. 5. Ratio of the actual dendrite tip radius as calculated from the phase field model to that calculated from the LKT model on the basis on constant σ^*, displayed as a function of Mc_∞. Note that for each of the four undercoolings displayed the value of σ^* to be used in the analytical model is obtained from the phase-field model at Mc_∞. = 0.02, where the ratio is, by definition, 1.

Figure 1

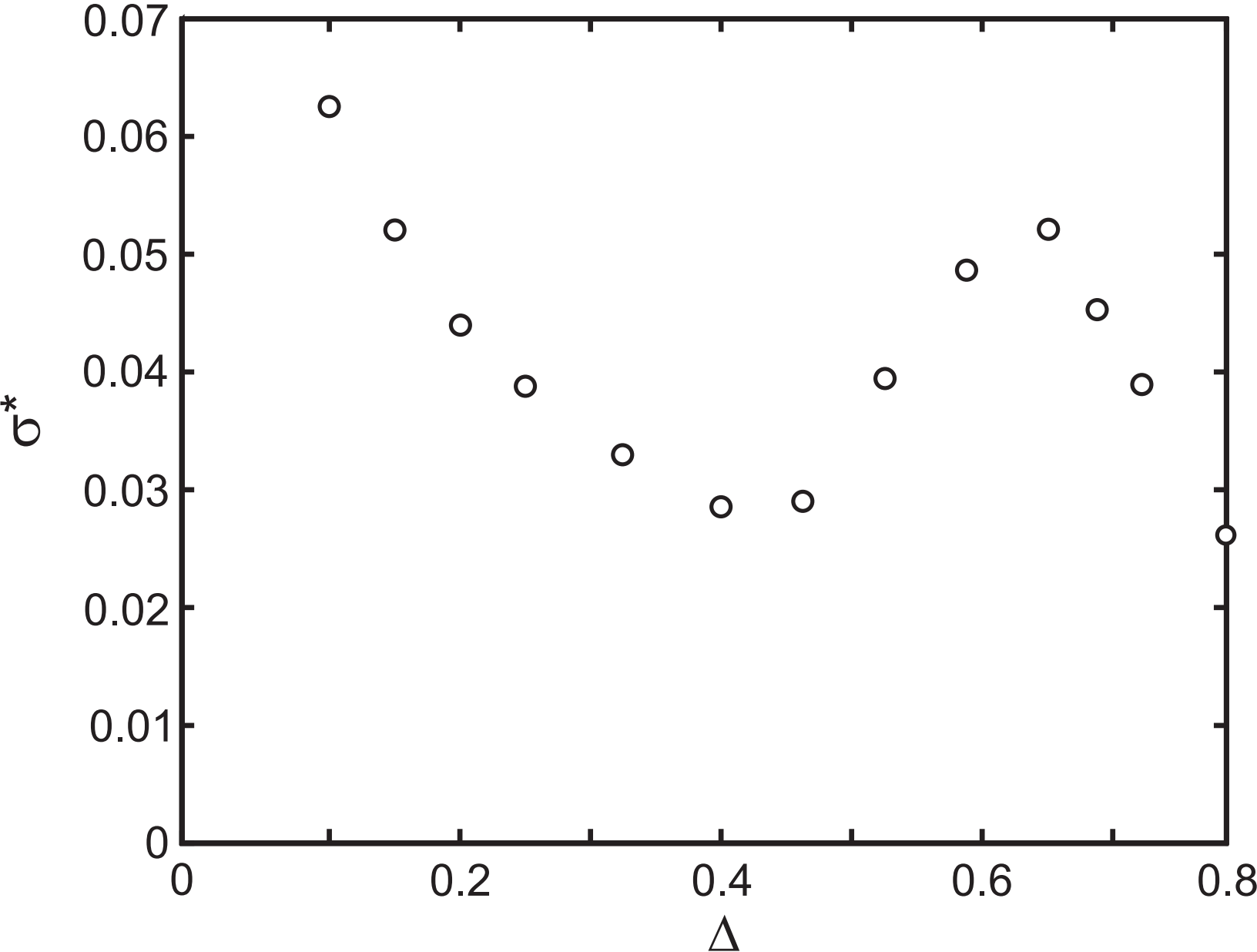

Figure 2

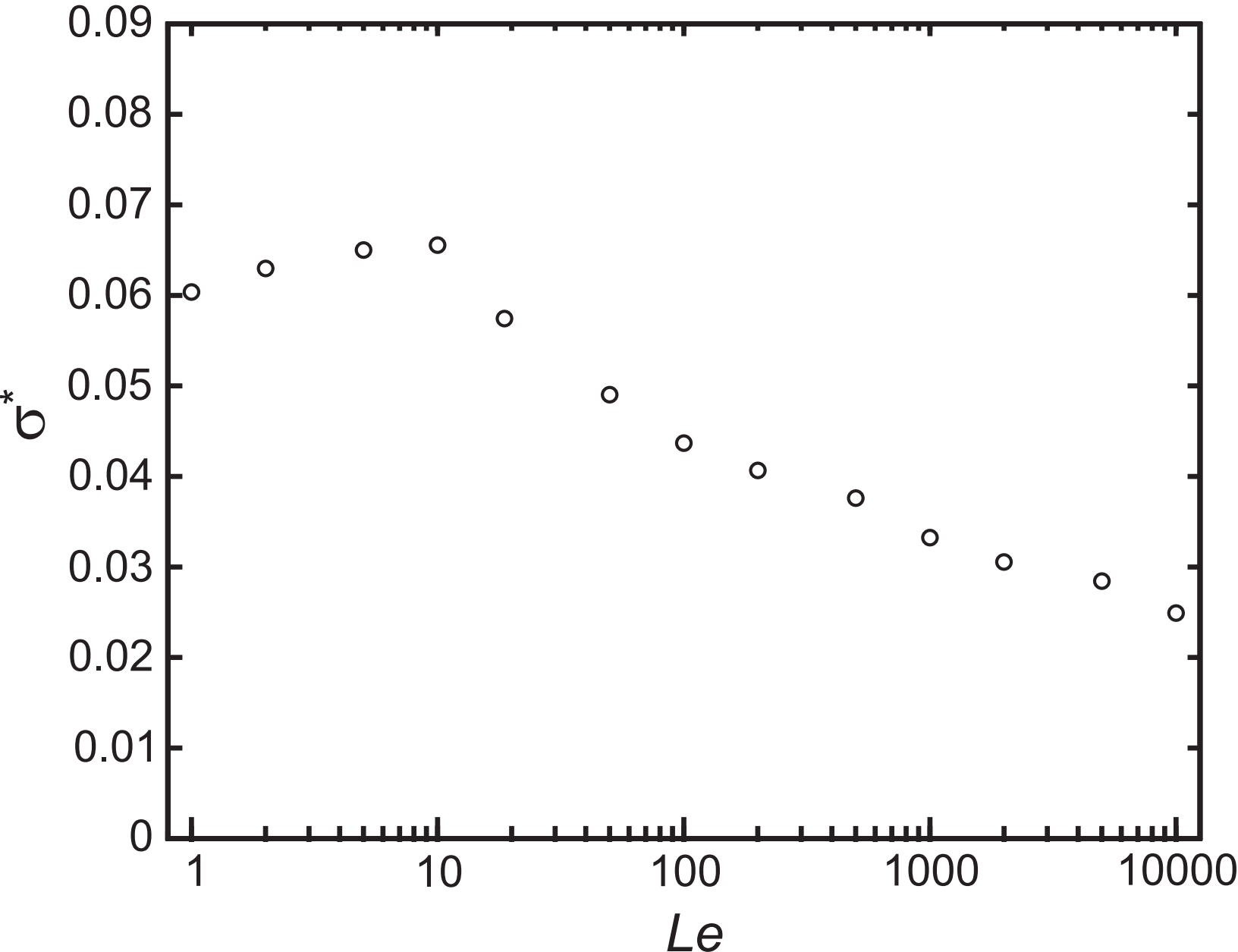

Figure 3

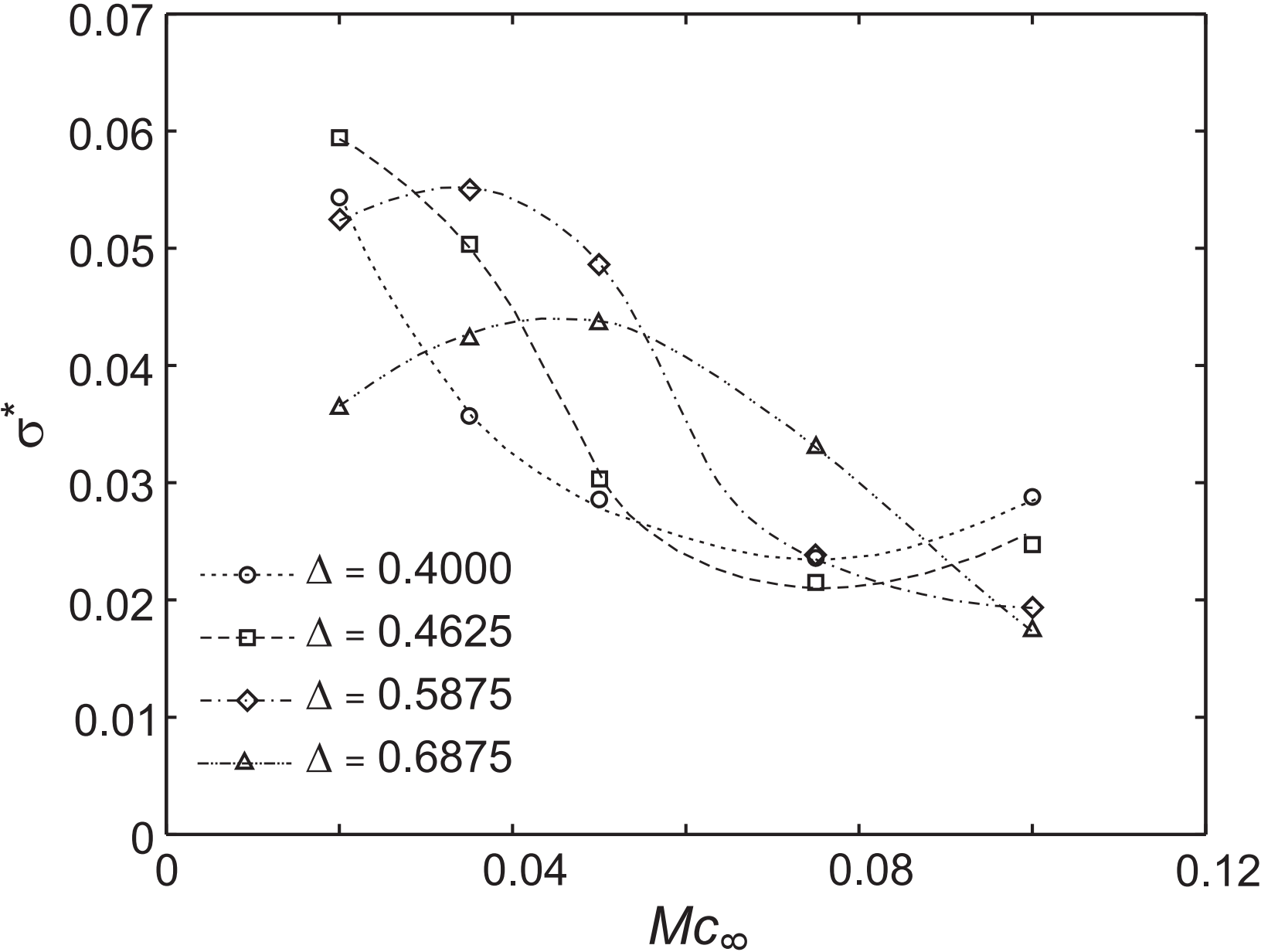
0.07
0.06
0.05
0.04
0.03
0.02
0.01
0
*b
0
0.04
0.08
0.12
Mc∞
Δ = 0.4000
Δ = 0.4625
Δ = 0.5875
Δ = 0.6875

Figure 4

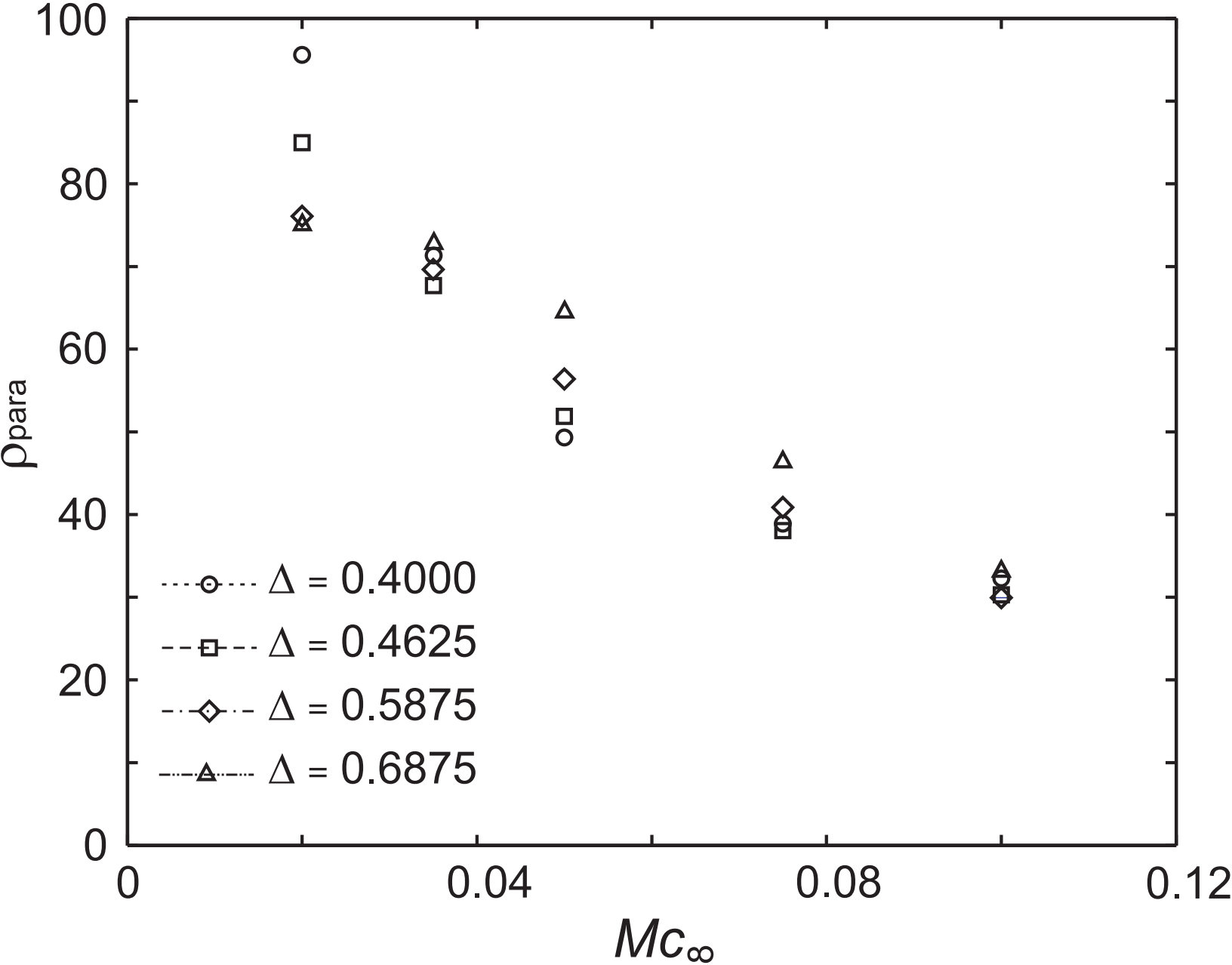
100
80
60
40
20
0
0
0.04
0.08
0.12
ρ_{para}
Mc_∞
Δ = 0.4000
Δ = 0.4625
Δ = 0.5875
Δ = 0.6875

Figure 5

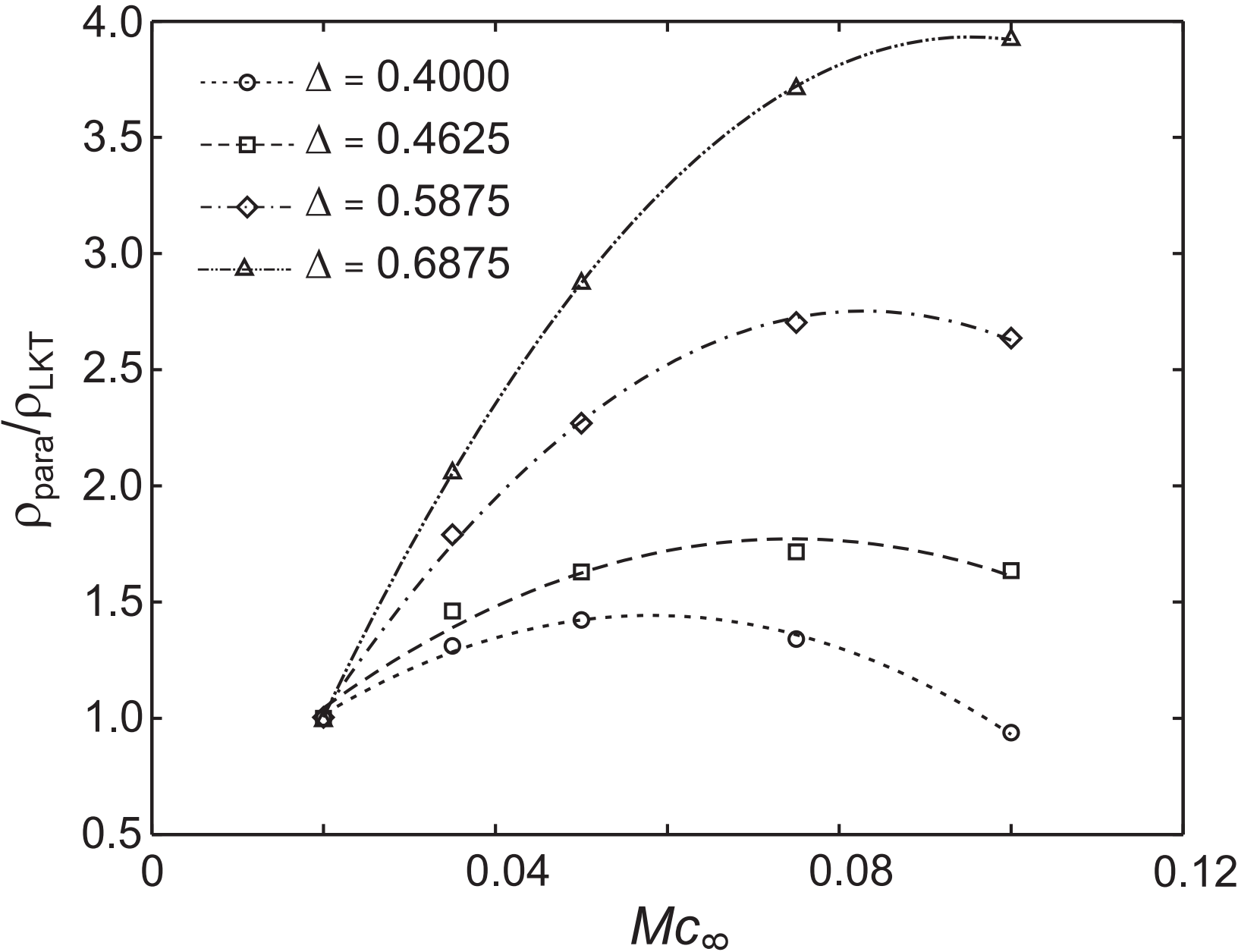
Δ = 0.4000
Δ = 0.4625
Δ = 0.5875
Δ = 0.6875
4.0
3.5
3.0
2.5
2.0
1.5
1.0
0.5
0
0.04
0.08
0.12
ρpara/ρLKT
Mc∞